Available online at www.sciencedirect.com
SCIENCE DIRECT®
Journal of Nuclear Materials 337–339 (2005) 515–519
journal of nuclear materials
www.elsevier.com/locate/jnucmat

Local effects of gas fuelling and their impact on transport processes in the plasma edge of the tokamak TEXTOR

B. Unterberg [a,*], S. Brezinsek [a], G. Sergienko [a], C.C. Chu [b], P. Dumortier [c], J.D. Hey [b], D. Kalupin [a], A. Kreter [a], M. Lehnen [a], A.M. Messiaen [c], Ph. Mertens [a], A. Pospieszczyk [a], U. Samm [a], B. Schweer [a], M.Z. Tokar' [a], G. Van Wassenhove [c], the TEXTOR-team

[a] *Institut für Plasmaphysik, Forschungszentrum Jülich GmbH, Trilateral Euregio Cluster, EURATOM-Association, D-52425 Jülich, Germany*
[b] *School of Pure and Applied Physics, University of KwaZulu-Natal, Howard College Campus, Durban 4041, South Africa*
[c] *Laboratoire de Physique des Plasmas/Laboratorium voor Plasmafysica, ERM/KMS, Trilateral Euregio Cluster, EURATOM-Association, B-1000 Brussels, Belgium*

Abstract

Deuterium fuelling through a carbon test limiter has been applied to maximize the plasma density in the Radiative Improved Mode. The impact of the fuelling on the local plasma edge properties has been investigated, by analyzing the spectral emission of both deuterium atoms and molecules, which indicates the creation of a cold and dense plasma cloud with a local electron density at the last closed flux surface up to 8×10^{19} m^{-3}, about 4 times higher than the electron density far away from the puffing location at the same plasma radius. The local electron temperature decreases to less than 10 eV. The experimental data can be reproduced by a model for the development of the cold plasma cloud and the critical fuelling rate to initiate the process based on the heat balance in the cloud. The correlation of the resulting local perturbation with the global confinement properties is discussed.

PACS: 52.25.Ya; 52.25.Fi; 52.40.Hf; 28.52.Cx
Keywords: Energy confinement; Gas injection and fuelling; Hydrogen; Spectroscopy; TEXTOR

1. Introduction

The application of strong gas fuelling in improved confinement regimes, to obtain high plasma densities close to operational limits in fusion devices, is usually connected with a severe degradation of the energy confinement (cf. discussion in [1] and references therein). This phenomenon can also be observed at the tokamak

* Corresponding author. Tel.: +49 2461 61 4803; fax: +49 2461 61 5452.
E-mail address: b.unterberg@fz-juelich.de (B. Unterberg).

0022-3115/$ - see front matter © 2004 Elsevier B.V. All rights reserved.
doi:10.1016/j.jnucmat.2004.09.041

TEXTOR where, in plasmas with a radiating boundary at densities around or even higher than the empirical Greenwald limit, improved energy confinement (Radiative Improved Mode (RI-mode) [2]) can only be achieved with moderate gas fuelling [3,4].

With the help of the RITM code the confinement degradation occurring with strong fuelling could be modeled and explained by a re-appearance of ion temperature gradient driven (ITG)-modes, which initially are reduced in the transition from L- to RI-mode, if the particle transport at the edge is notably increasing [5]. Such an enhanced transport has been associated with drift resistive ballooning modes growing during the formation of a cold and dense plasma cloud at the location of the strong gas injection [6,7]. While the electron densities and temperatures have been measured by spectroscopic means in divertor plasmas [8,9], we will investigate the local effects of gas fuelling for different injection rates on the basis of spectroscopic methods, and relate these findings to transport properties at the plasma edge and the overall plasma performance in the RI-mode discharges.

2. Experimental set-up

The experiments reported here were performed in the medium-sized tokamak TEXTOR ($R = 1.75$ m, $a = 0.46$ m) at standard values of plasma current ($I_P = 400$ kA) and toroidal field ($B_T = 2.25$ T). The plasma was heated by neutral beam and by ion cyclotron resonance waves at a total power of $P_{aux} = 3.0$–3.5 MW and had a density close to the Greenwald limit (here $\bar{n}_{GW} = 6.0 \times 10^{19}$ m^{-3}). A transition to the RI-mode is obtained by feedback controlled neon seeding. After the transition to improved confinement, deuterium has been fuelled into these discharges through a carbon test limiter positioned in the limiter lock of TEXTOR (0–30 mm behind the last closed flux surface at $a = 0.46$ m) well equipped with spectroscopic diagnostics (cf. [10]). The atomic deuterium injection rate has been varied between 10^{20} s^{-1} and 3×10^{21} s^{-1}.

The spectral emission of both deuterium atoms and molecules is measured at the puffing location. The intensity of the Fulcher-α band is measured with a 0.8 m spectrometer in Littrow mounting (resolving power $\lambda/\Delta\lambda = 13\,000$). The rotational temperature T_{rot} of deuterium molecules, occupying the $3P^3\Pi_u$ electronic state, has been determined by means of a Boltzmann-plot, where the first lines of the Q-branch ($Q2$–$Q8$) of the first diagonal vibrational transition (0–0) have been used. T_{rot} has been found to increase mainly with the electron density n_e for typical conditions at the last closed flux surface of TEXTOR (electron temperature $T_e = 30$–100 eV, $n_e = 0.1$–1.5×10^{19} m^{-3}) [11]. This behavior can be attributed to an increase of the population of the upper electronic level of the transition proportional to n_e.

A thermal Helium beam distant from the puffing location [12] has been used to measure n_e and T_e profiles at the edge. To determine the local electron density at the puffing location we applied the relation between rotational temperature and density under conditions of strong gas fuelling. The local electron temperature has been estimated assuming a constant pressure along the field lines.

The spectral distribution of D_α at the fuelling location is measured with a high resolution Echelle spectrometer in Littrow mounting ($\lambda/\Delta\lambda = 87000$, used in 37th order). The composition of the spectrum has been analyzed in detail in [13]. A broad pedestal represents a charge exchange component revealing the local deuteron temperature. A central component at a low atomic radiator temperature labelled 'cold' may be interpreted as evidence for electron impact-induced molecular dissociation, coupled with dissociative excitation, which leads to Franck–Condon energies of 0.3 eV. This process requires a threshold energy of 17 eV for the incident electron. Further possible processes leading to comparably low kinetic energies of the atoms are collision-induced dissociative excitation into the level $n = 2$ of the deuterium atoms and dissociative ionization with thresholds for the electron energy of 14.6 eV and 18 eV (cf. [13] and references therein). The absence of this 'cold' component can be related to thermal electron energies below the corresponding thresholds. Higher atomic radiator temperatures are obtained as a result of direct molecular dissociation into ground-state atoms with a lower threshold energy of 8.876 eV, which yields a Franck–Condon energy of 2.2 eV/atom and corresponding radiator temperatures of 1.5 eV (denoted as 'lukewarm'). Both components can be heated in ion–atom collisions, but the 'cold' and 'lukewarm' components are expected to remain distinguishable under typical plasma conditions in TEXTOR [13].

Furthermore, we measured the intensity of high-n Balmer lines (D_ϵ, D_{8-2} and D_{9-2}) by means of a spectrometer in Czerny–Turner mounting with $\lambda/\Delta\lambda = 8000$. The lines of sight of the three spectrometers mentioned so far view the gas injection zone perpendicular to the toroidal magnetic field. While the first two collect the light integrated from an observation volume extending radially from $r = 0.48$–0.43 m, the latter reveals a radially resolved intensity profile from $r = 0.49$–0.39 m with a resolution of 0.2 mm. The two dimensional pattern of D_α emission in a toroidal–radial plane is measured by means of a CCD camera equipped with an interference filter at a wavelength of $\lambda = 656.3$ nm with a width of $\Delta\lambda = 3$ nm.

3. Results and discussion

A first indication for the formation of a cold and dense plasma cloud is based on the correlation between the elec-

tron density at the edge and the rotational temperature of D_2 molecules. We compared the rotational temperatures with the electron density measured far away from the puffing location, n_e, upstream, for a large number of discharges at various time intervals (cf. Fig. 1(a)). Here the external fuelling rate is used as a parameter. While for no, or very small, injection rates (triangles) we recover the linear correlation already obtained in [11], for higher puffing rates, the local rotational temperature is much larger. We attribute this fact to a local increase of the electron density because of the strong local plasma source. We quantify the perturbation by extrapolating the linear relation, found for the case of no gas injection. As a function of the gas injection rate we find a local increase of the density up to 8×10^{19} m^{-3} as shown in Fig. 1(b). This is four times the density measured upstream. If we further assume a constant pressure along the field lines, we can find a local cooling of the plasma by the same factor yielding electron temperatures down to less than 10 eV.

This observation alone does not strictly prove the formation of the cold plasma cloud as the relation between T_{rot} and n_e has not been established in [11] up to the extreme conditions deduced by extrapolation in Fig. 1. Therefore, we turn to the analysis of the spectral shape of D_α emission from the injection zone (cf. [13]). We observe a clear broadening of the spectra in the case of strong gas injection (Fig. 2(b)) in comparison with the situation prior to the gas injection (Fig. 2(a)). Fig. 2(c) illustrates this finding quantitatively, giving the results of the fitting procedure with respect to the temperatures of the 'cold' and 'lukewarm' components and their contribution to the total emission. During the gas injection the percentage of the 'cold' component is significantly reduced while the fraction of the 'lukewarm' increases at the same time (dotted curves). The intensity ratio $I_{cold}/I_{lukewarm}$ decreases from 0.6 to 0.14. We conclude from this change that the importance of the 'cold' component is diminished because the local electron temperature is markedly reduced such that it approaches the threshold for the production of Franck–Condon atoms with energies of around 0.3 eV ($T_e \approx 12$ eV). While the small 'cold' contribution is heated up significantly by collisions, the plasma cooling is further confirmed by the evolution of the temperature of the charge exchange (CX) components as deduced from the far wings of the spectrum, which are subtracted prior to the fitting of the 'cold' and 'lukewarm' components and give ion temperatures down to 15 eV during the puff.

The local cooling derived indirectly from the pressure balance along the field lines is supported by the fact that the D_α emission of the cloud becomes toroidally asymmetric under the conditions of the strongest perturbations. We attribute this finding to the drag exerted onto the atoms during the time until they are ionized, indicating a reduction of the electron temperature below the ionization threshold. On the other hand we observe no significant population of the upper Rydberg states of high-n Balmer lines (D_ϵ, D_{8-2} and D_{9-2}) by recombination comparing a spectrum during strong gas fuelling to the one obtained during a multi-faceted asymmetric radiation from the edge (MARFE) at the high field side with temperatures as low as 1 eV [14]. From this, we conclude that the electron temperatures are still in excess of about 5 eV.

Next we want to compare the local densities and temperatures at the gas fuelling zone to results from a model based on a local power balance at the puffing location [6]. It considers deuterium atoms only, disregarding any molecular processes. The power lost from the injection zone is related to the injection rate Γ_{gas} as:

$$Q_{loss} = \Gamma_{gas}(E_i + 3/2T_cA^* + 5T_c). \quad (1)$$

The first term, E_i, denotes the energy lost by ionization and excitation processes, the second term refers to the heating of neutrals by charge exchange and the last

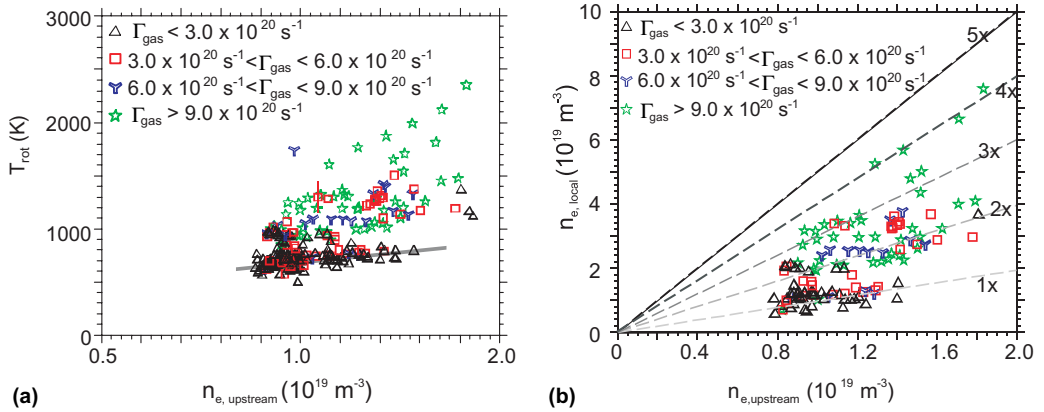

Fig. 1. (a) Rotational temperature of D_2 molecules and (b) local density deduced from rotational temperatures as a function of the electron density remote from the injection zone for various injection rates.

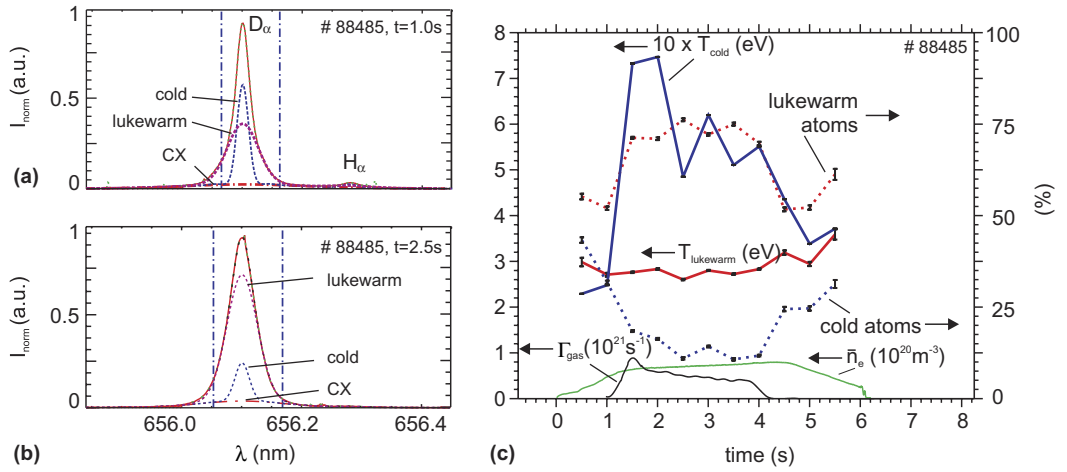

Fig. 2. Normalized intensity of D_α spectra measured (a) before the start of external deuterium fuelling, (b) during external fuelling with an injection rate of $\langle \Gamma_{\mathrm{gas}} \rangle = 7 \times 10^{20}\ \mathrm{s}^{-1}$, (c) time evolution of radiator temperatures and contribution to total intensity in comparison to fuelling rate and line averaged central electron density.

term to the energy outflow with the ions and electron generated in the ionization processes. A^* is called the plasma albedo leading to an amplification of the neutral influx to the cloud by charge exchange by the factor $(1 - R \cdot A^*)^{-1}$ with R the local recycling coefficient. T_c is the temperature in the plasma cloud, n_c the local density. The heat flux to the cloud is predominantly given by parallel heat conduction. It is approximated by a '2-point model' connecting the plasma parameters in the cloud and the upstream values

$$Q_{\mathrm{heat}} = \frac{2\kappa_0}{7L} S_c \left(T_u^{7/2} - T_c^{7/2}\right). \tag{2}$$

Here, $\kappa_0 = 10^{22}\ \mathrm{m}^{-1}\ \mathrm{s}^{-1}\ \mathrm{eV}^{-5/2}$ denotes the electron heat conductivity coefficient, $L = 4\pi^2 aR/(2\delta_c)$ is the distance over which the cloud influences the edge plasma and δ_c the cloud extension. S_c is the area of the cloud perpendicular to the magnetic field (2 sides) and T_u the upstream temperature. Local and upstream parameters are connected via the assumption of a constant pressure ($n_u T_u = n_c T_c$). Fig. 3 shows a comparison between experimental data and modelling results for the local electron density (lower triangles and solid line) and the local electron temperature (upper triangles and dashed line). Although the model uses simplifying assumptions in many respects, it can well reproduce the critical puffing rate to form the cold and dense plasma cloud.

Finally, we discuss the impact of the external gas fuelling on the edge transport and the overall confinement properties of the plasma. Caused by the significant increase of the collisionality at the puffing location (ν^* increases by an order of magnitude to values as high as 250) we expect a substantial increase of drift resistive ballooning modes as predicted in [7]. Experimentally, a marked increase of density fluctuations measured by

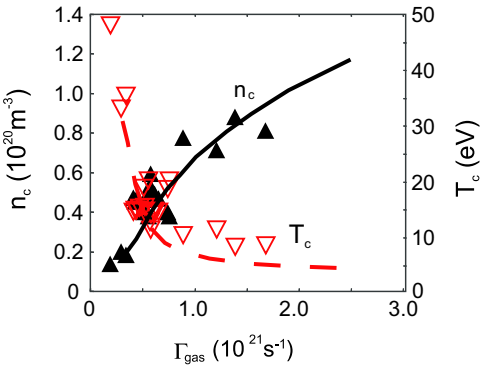

Fig. 3. Impact of external gas fuelling on local density and temperature in experiment and model (lines show results from modelling with $T_u = 50$ eV, $n_u = 1.5 \times 10^{19}\ \mathrm{m}^{-3}$, triangles denote experimental data corresponding within ±15% to the input data of the model).

reflectometry just inside the LCFS is observed under conditions of strong gas fuelling [5] which at least qualitatively supports our picture of an increased edge transport. As a result, we also observe remote from the fuelling location an increase of the electron density (cf. Fig. 1(b)), of the total recycling flux at the plasma facing components and of the neutral pressure close to the wall.

In Fig. 4 the energy confinement time normalized to the scaling for the RI-mode ($\tau_{E,RI} = \mathrm{const.} \cdot \bar{n}_e / n_{GW} P_{aux}^{-2/3}$ [2]) is shown as a function of the Greenwald number ($\bar{n}_e / n_{GW}$). The data essentially align along two distinct branches, a high performance branch and a branch showing a degradation to L-mode confinement. We calculated the total influx at the puffing location (i.e. the external fuelling rate amplified by the subsequent local-

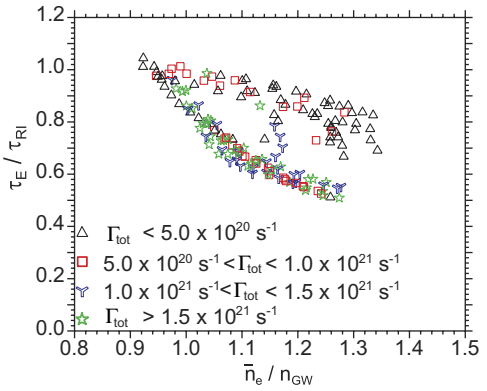

Fig. 4. Global energy confinement time as a function of normalized density in discharges with a radiating plasma boundary, different symbols denote different values of the total neutral influx to the injection zone.

ized recycling flux) and used it as the discriminating parameter. The local perturbation is well correlated with the global confinement properties characterized by the energy confinement time. The increase of edge transport owing to the perturbation leads to a more effective impurity screening. If the impurity content in the plasma bulk is reduced too strongly, a confinement degradation back to L-mode levels takes place through the re-appearance of ITG modes as discussed in [5].

4. Summary and conclusions

It has been shown that strong external gas fuelling into RI-mode discharges at the tokamak TEXTOR leads to the formation of a cold and dense plasma cloud with electron temperatures below 10 eV and densities up to 8×10^{19} m^{-3} at the LCFS ($a = 0.46$ m). The development of the localized recycling zone and the critical fuelling rates to initiate the process observed experimentally can be reproduced by a simple model based on a heat balance for the cloud. The global confinement properties of the RI-mode at densities above the Greenwald limit is found to be crucially dependent on the extent of the resulting local perturbation.

References

[1] ITER Physics Basis Editors and ITER Physics Expert Groups Chairs and Co-Chairs, Nucl. Fusion 39, 2137 (1999).
[2] R.R. Weynants et al., Nucl. Fus. 39 (1999) 1637.
[3] G. Mank et al., Phys. Rev. Lett. 84 (2000) 2312.
[4] J. Ongena et al., Phys. Plasmas 8 (2001) 2188.
[5] D. Kalupin et al., Plasma Phys. Control. Fus. 43 (2001) 945.
[6] M.Z. Tokar', Plasma Phys. Control. Fus. 35 (1993) 1119.
[7] M.Z. Tokar' et al., Proceedings of the 29th EPS Conference on Plasma Phys. Control. Fus. Montreux, 17–21 June 2002, ECA, Vol. 26B, P-1.097 (2002).
[8] B.L. Welch et al., Phys. Plasmas 2 (1995) 4246.
[9] U. Fantz, B. Heger, D. Wünderlich, Plasma Phys. Control. Fus. 43 (2001) 707.
[10] S. Brezinsek et al., J. Nucl. Mater. 313–316 (2003) 967.
[11] S. Brezinsek et al., Contrib. Plasma Phys. 42 (6–7) (2002) 668.
[12] B. Schweer et al., J. Nucl. Mater. 192–196 (1992) 174.
[13] J.D. Hey, C.C. Chu, Ph. Mertens, S. Brezinsek, B. Unterberg, J. Phys. B: At. Mol. Opt. Phys. 37 (2004) 2543.
[14] G. Sergienko et al., J. Nucl. Mater. 290–293 (2001) 720.